EurJOC European Journal of Organic Chemistry

FULL PAPER

DOI: 10.1002/ejoc.201200644

Fused Arene Ring Construction Around Pyrrole To Form 4,7-Disubstitued Indole

Elżbieta Nojman,[a] Lechosław Latos-Grażyński,*[a] and Ludmiła Szterenberg[a]

Keywords: Heterocycles / Dimerization / Rearrangement / NMR spectroscopy

A method for synthesizing 4,7-diarylindoles and 4,7-di(thien-2-yl)indole by applying a strategy where the fused benzene ring was built on an existing pyrrole in an acid-catalyzed rearrangement of 1,4-diaryl-1,4-di(pyrrol-2-yl)but-2-yne and 1,4-di(pyrrol-2-yl)-1,4-di(thien-2-yl)but-2-yne, respectively, is presented. In the presence of TFA (30 equiv.), 4,7-diarylindoles undergo thermodynamically equilibrated dimerization at 240 K as determined by ^{1}H NMR spectroscopy and substantiated by DFT calculations.

Introduction

The indole unit is present in a multiplicity of natural compounds, many of which reveal significant physiological activities. Noticeably, the indole ring system can be classified as a fundamental structural component in a large variety of therapeutic agents.[1–7] The recent progress of indole chemistry can be also related to materials chemistry, as several indole-containing materials have been explored. For instance, materials that contain indole as the functional unit can act as nonlinear optical (NLO) chromophores[8,9] or can be applied as fundamental building blocks for blue[10] or red[11] electroluminescent materials. Indole-based light-emitting oligomers containing indole moieties with arylene-vinylene and aryl bridges have been reported as well.[12] Branched diphenylsilane derivatives containing electronically isolated indolyl moieties act as host materials for organic blue-light-emitting diodes.[13] Finally, copolymers containing indole-related units with fine-modulated optical and electrical properties are promising candidates for photovoltaic application.[14,15] The fundamental role in all areas outlined above creates unceasing demand for the development of general, flexible, and especially regioselective synthetic methods of such a structural moiety.[7,16–23]

According to recently proposed classification by Taber and Tirunahari, it is apparent that every indole synthesis fits one of the nine strategic approaches.[23] In fact, in the simplified view applied here for the convenience of further discussion, these nine well-defined strategies can be gathered into three major groups. Thus, in the first group, the pyrrolic ring is built on an existing benzene or cyclohexane ring. The recently reported synthesis of 4,7-diarylindoles, obtained in search of an indole-based fluorescent chemosensor for iodide ions, falls in this category. In this case, 4,7-diarylindoles were synthesized starting from 1,4-dibromobenzene to afford 4,7-dibromoindole to be used as an appropriate substrate in Suzuki coupling.[24] In the second set, the fused benzene ring is built on an existing pyrrole. Finally, in the third group, both rings are constructed simultaneously. Actually, the majority of the reported syntheses start with benzene-type substrates, and evidently, they belong to the first category.[7,16–23] The alternative procedure (the van Leusen strategy), which uses a pyrrole ring as the "template"-like structure (in fact applicable in this study), is definitely less common[23,25,26] and includes the recently reported palladium-catalyzed oxidative coupling of 3-substituted pyrrole with alkynes to form 4,5,6,7-tetraphenylindole[27,28] or the Lewis acid catalyzed [4+2] benzannulation between enynal units and enols or enol ethers to form 4,6-disubstituted or 4,5,6-trisubstituted indoles.[26]

Herein, we report an efficient synthesis of 4,7-disubstituted indoles by fused arene ring construction around a pyrrole by applying a catalyzed rearrangement of 1,4-diaryl-1,4-di(pyrrol-2-yl)but-2-yne or 1,4-di(pyrrol-2-yl)-1,4-di(thien-2-yl)but-2-yne. Subsequently, the acid-induced reversible dimerization was explored by applying a combined NMR/DFT approach.

Results and Discussion

Syntheses of 1,4-Diaryl-1,4-di(pyrrol-2-yl)but-2-yne and 1,4-Di(pyrrol-2-yl)-1,4-di(thien-2-yl)but-2-yne

A starting step in the synthesis of 4,7-diarylindoles **1a**–**c** and 4,7-di(thien-2-yl)indole **1d** is the formation of 1,4-diaryl-1,4-di(pyrrol-2-yl)but-2-ynes **2a**–**c** and 1,4-di(pyrrol-2-yl)-1,4-di(thien-2-yl)but-2-yne **2d**. Previously, we used these ethyne derivatives for introducing the ethyne unit into the porphyrin-like skeleton 20-thiaethyneporphyrin.[29]

[a] Department of Chemistry, University of Wrocław,
14 F. Joliot-Curie St., 50 383 Wrocław, Poland
Fax: +48-713282348
E-mail: lechoslaw.latos-grazynski@chem.uni.wroc.pl

Supporting information for this article is available on the WWW under http://dx.doi.org/10.1002/ejoc.201200644.

1,4-Diaryl-2-butyne-1,4-diols **3a**–**c** and 1,4-di(thien-2-yl)-2-butyne-1,4-diol **3d** were obtained by applying the standard approach in the reaction of aryl aldehyde or thiophene-2-carbaldehyde with the Grignard reagent BrMgC≡CMgBr in THF.[30,31] Subsequently, the modified Nicholas reaction was applied (Scheme 1).[32–38] A direct reaction between 1,4-diaryl-2-butyne-1,4-diol **3a**–**c** or 1,4-di-(thien-2-yl)-2-butyne-1,4-diol **3d** and pyrrole (in excess) catalyzed with TFA (trifluoroacetic acid) failed to produce **2a**–**c** or **2d** but produced trace amounts of 4,7-disubstituted indoles **1**. Subsequent reaction with pyrrole as a nucleophile followed by decomplexation afforded substituted alkynes, that is, **2a**–**d**. The yields (ca. 30%) of this step resembles that of originally reported **2a**.[29]

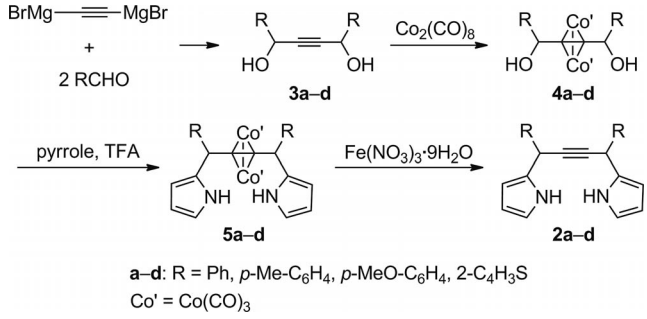

Scheme 1. Synthesis of 1,4-di(pyrrol-2-yl)-2-butynes **2a**–**c** and **2d**.

Synthesis of 4,7-Disubstituted Indoles

Initially, compounds **2** were used as the fundamental substrate in the synthesis of 20-thiaethyneporphyrin by using a simple modification of the "3+1" approach[39,40] by applying $BF_3{\cdot}OEt_2$ as a catalyst, whereas **2** was considered as the ethyne analogue of tripyrrane. In the course of the reaction, 4,7-diarylindoles were identified as a specific quite disturbing side product.

In this study, the addition of TFA to a solution of **2** in $CDCl_3$ was monitored by ^1H NMR spectroscopy, which provided spectroscopic evidence that under such conditions 4,7-diarylindole was immediately formed as the sole identified product of the conversion. Consequently, we decided to optimize this route as a suitable procedure to generate 4,7-disubstituted indoles. In fact, on the synthetic scale 1,4-diaryl-1,4-di(pyrrol-2-yl)but-2-yne [1,4-di(pyrrol-2-yl)-1,4-di(thien-2-yl)but-2-yne] in the presence of TFA converts preferably into 4,7-diarylindole [4,7-di(thien-2-yl)indole] (Scheme 2). Chromatography yielded 4,7-disubstituted indoles **1** readily identified by NMR spectroscopy. The molecular structure of **1c** was determined by X-ray diffraction studies (Figure 1). The bond lengths and bond angles resemble those reported for other indole derivatives.[41,42]

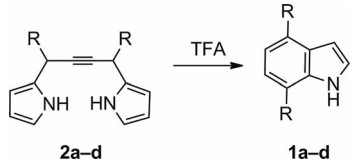

Scheme 2. Synthesis of 4,7-di(thien-2-yl)indole.

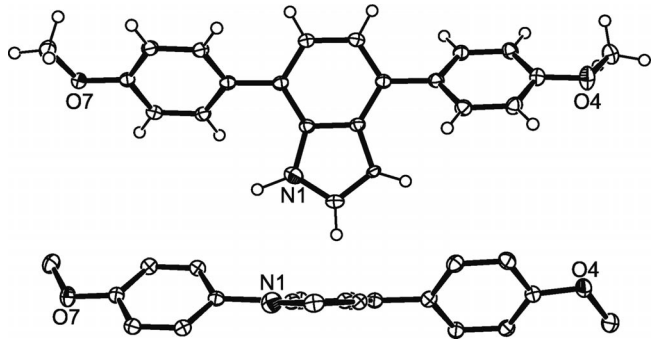

Figure 1. Molecular structure of **1c** (top: perspective view, bottom: side view). The thermal ellipsoids represent 50% probability. The dihedral angles between aryl groups and the indole unit are –48.1° (C5–C4–$C4_{ipso}$–$C4_{ortho}$) and –42.7° (C6–C7–$C7_{ipso}$–$C7_{ortho}$).

Suggested Mechanism

For the mechanism of formation of 4,7-disubstituted indoles **1** (Scheme 3), we suggest that TFA acidolysis of **2** via formation of **2**-H^+[43–45] affords transient reactive cationic species **2**-1. Subsequently, the process involves a deep reorganization of propargyl cation **2**-1, which may undergo necessary dual hydrogen migration of the atoms originally located at the 1,4-positions of **2**. This transformation generates substituted 1,3-diene cation **2**-2, which is suitably prearranged for intramolecular electrophilic attack at the adjacent pyrrole to close the six-membered ring.

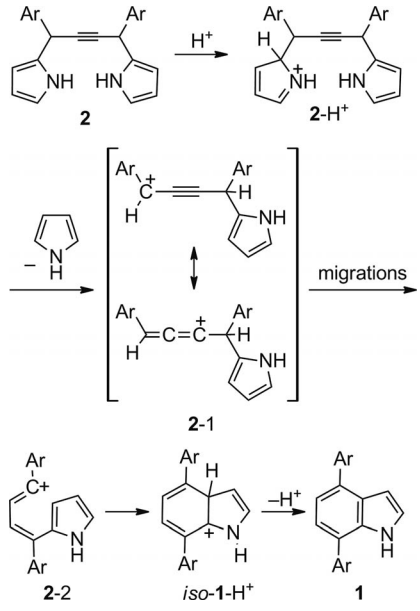

Scheme 3. Mechanism of transformation.

To validate the mechanism of formation, an identical reaction was carried out by using [D]TFA instead of TFA and [D_2]dichloromethane instead of dichloromethane. The

formation of 1,3-dideuterioderivative **1a**-d_2 was solely observed. Thus, the 5-H and 6-H hydrogen atoms of **1a** are definitely provided by an intramolecular process as postulated above. Deuteration at the N1 and C3 positions reflects the typical acid–base chemistry exhibited by indoles in general.[46] Thus, addition of [D]TFA results eventually in replacement of hydrogen by deuterium in the specified positions according to that shown in Scheme 4 (Supporting Information, Figure S28).

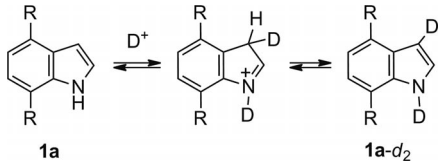

Scheme 4. Deuteration of 4,7-diarylindole.

Dimerization

Monoprotonated indoles **1**-H$^+$ have not been directly observed by ^{1}H NMR spectroscopy (Figure 2). Lowering of the temperature favors the formation of N-protonated 2-(3-indolyl)indoline **6**-H$^+$ (Scheme 5). The dimerization of **1** follows the pattern reported for regular indole,[47] which suggests increased electrophilicity at the C2 position as a result of protonation at C3.

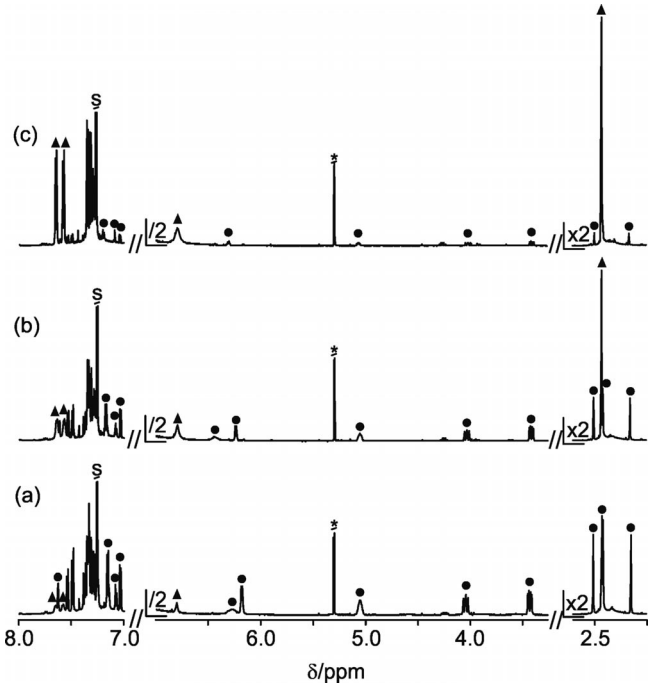

Figure 2. Reversible dimerization of 4,7-di(*p*-tolyl)indole **1b** (30 equiv. of TFA added, $CDCl_3$). Labeling of the representative resonances: triangles **1b**, circles **6b**-H$^+$: (a) 260 K, (b) 280 K, (c) 300 K. The intensity of the peaks in all traces is standardized with respect to the solvent. The resonance marked with an asterisk is assigned to residual dichloromethane.

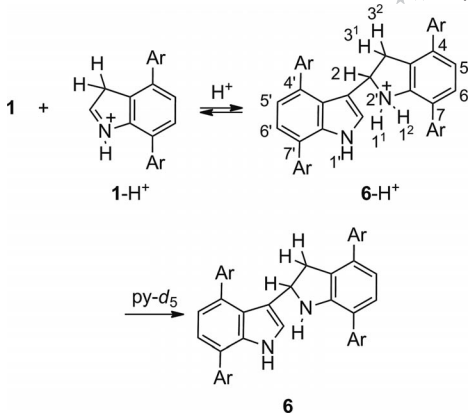

Scheme 5. Dimerization of 4,7-diarylindole.

The dimerization requires 30 equiv. of TFA and was accomplished usually at 240 K. Systematic increase in the temperature results in recovery of 4,7-diarylindole **1**. In fact, indole **1** and protonated 2-(3-indolyl)indoline **6**-H$^+$ are in thermodynamic equilibrium as demonstrated by the thermal reversibility of the process with preservation of the **1**/**6**-H$^+$ molar ratio for the given acid concentration and temperature (1:9, 240 K; 9:1, 300 K, 30 equiv. of TFA). Significantly, neutralization of **6**-H$^+$, monitored by ^{1}H NMR spectroscopy, carried out by addition of 100 equiv. of [D_5]-pyridine at 240 K affords free base **6**, which under such conditions remain the sole species in the temperature range 240–300 K. The dimerizations of indoles already reported follow the route shown in Scheme 5.[47–52]

The identity of **6b**-H$^+$ was confirmed by high-resolution mass spectrometry and NMR spectroscopy. Thus, the assignments of the resonances of **6b**-H$^+$ (Figure 3) were made on the basis of the relative intensities and detailed 2D NMR studies (COSY, NOESY, ROESY, HMQC, HMBC) carried out at 260 K in [D]chloroform, where the conversion was practically complete. The ^{1}H NMR spectrum of **6b**-H$^+$ con-

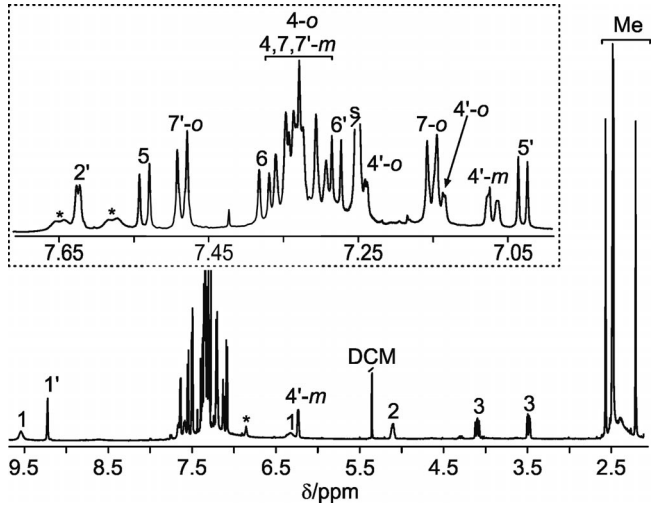

Figure 3. ^{1}H NMR spectrum of **6b**-H$^+$ ([D]chloroform, 260 K). Numbering: see Scheme 5. Insets demonstrate the crowded 6.9–7.7 ppm region. Resonances of **1b** are marked with asterisks.

tains two subsets of resonances readily assigned to 4,7-diarylindole and 2,3-dihydroindole (indoline) related moieties through relays of COSY (indole 1′-H ↔ 2′-H, 5′-H ↔ 6′-H, and 2,3-dihydroindole 1^1-H ↔ 1^2-H, 1^1-H ↔ 2-H, 2-H ↔ 3^1-H, 2-H ↔ 3^2-H, 3^1-H ↔ 3^2-H, 5-H ↔ 6-H).

The dimerization experiment carried out in the presence of [D]TFA afforded the derivative, whereas substitution by deuterium took place at C3, N1′, and N1 following in fact the deuteration pattern of 4,7-diarylindole discussed in detail above. Significantly, the complementary HSQC experiment allowed the unambiguous identification of the unique C2 resonance revealing its tetrahedral geometry consistent with the 63.1 ppm chemical shift. The straightforward assignment of the 2-H resonance presented above provided the initial step for the ^{1}H NMR spectroscopic analysis (Figure 3). Once assigned, this particular set of resonances was used as a starting point for the NOE studies. The fundamental relay of NOE connectivities is shown in Figure 4.

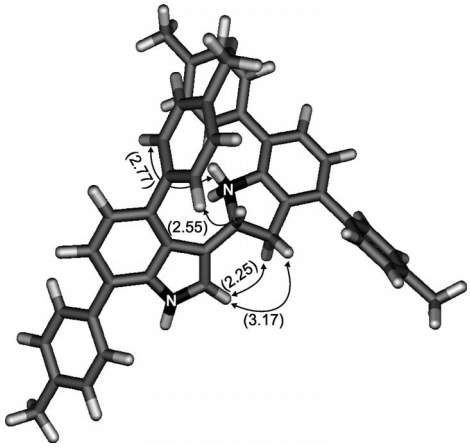

Figure 4. The established NOE connectivities for (**6b**-H$^+$)$_1$. The spatial proximities (in Å, from DFT optimized model) are in parentheses.

Noticeably, four different sets of *meso*-*p*-tolyl ring resonances were detected readily via COSY and NOESY, which correlated with particular methyl resonances. The detected differentiation of the *ortho* and *meta* resonances seen for 4′-*p*-tolyl, which is linked to the indole moiety, suggests that their rotation with respect to the C_{meso}–C_{ipso} bond is slow at 260 K, and obviously, **6b**-H$^+$ is not planar. In contrast, fast rotation was detected for the 7′-, 4-, and 7-*p*-tolyl groups, as documented by a single doublet for the *ortho* and *meta* positions in each case.

Two principal conformers of **6b**-H$^+$ can be readily distinguished by the C3–C2–C3′–C2′ dihedral angles (**6b**-H$^+$)$_1$: –4.7°; (**6b**-H$^+$)$_3$: –115.2° (Figure 5, Table 1). Considering in detail the spatial proximity of the 2-H-*o*-H_a(4′-Tol) (2.55 Å) and 1^1-H-*o*-H_b(4′-Tol) (2.77 Å) as found at the DFT-optimized structure of (**6b**-H$^+$)$_1$, one could expect the NOE cross-peaks, reflecting the coinciding dipolar coupling between the 2-H and 1^1-H hydrogen atoms, to *o*-H(4′-Tol). Consistently with the considered structure, only 3^1-H is close enough to produce the detectable dipolar 3^1-H-2′-H (2.25 Å) and 3^2-H-2′-H (3.17 Å) correlations (in parentheses the shortest H–H distances are given). These structural features have been reflected in the ROESY map by two well-defined cross-peaks (Supporting Information, Figure S29). Originally, the DFT model of the second rotamer (**6b**-H$^+$)$_3$ was also analyzed. One can readily demonstrate that the above-described fundamental connectivity pattern is not consistent with the geometry of (**6b**-H$^+$)$_3$. For instance, the fundamental 2-H-*o*-H(4′-Tol) dipolar correlation is not feasible in the second rotamer, as the optimized shortest distance equals 4.97 Å.

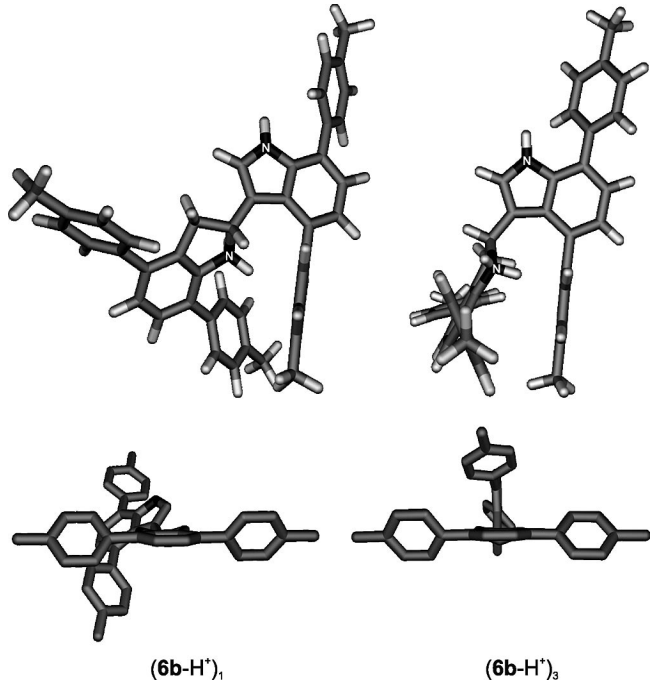

Figure 5. Geometries of (**6b**-H$^+$)$_1$ and (**6b**-H$^+$)$_3$ in a DFT optimization at the B3LYP/6-31G** level. Side projections emphasize the conformations of **6b**-H$^+$ with respect to the C2–C3′ bond (indoline unit in front).

Table 1. Selected dihedral angles for **6b**-H$^+$ rotamers.

Dihedral angle / °	Conformer			
	(**6b**-H$^+$)$_1$	(**6b**-H$^+$)$_2$	(**6b**-H$^+$)$_3$	(**6b**-H$^+$)$_4$
C3–C2–C3′–C2′	–4.7	–11.4	–115.2	–116.4
C5–C4–$C4_{ipso}$–$C4_{ortho}$	–52.0	–49.6	–43.3	–41.5
C6–C7–$C7_{ipso}$–$C7_{ortho}$	–48.3	51.3	–55.4	43.2
C5′–C4′–$C4'_{ipso}$–$C4'_{ortho}$	–67.1	–57.3	–95.7	–91.9
C6′–C7′–$C7'_{ipso}$–$C7'_{ortho}$	44.7	44.5	47.0	46.6

Significantly, the fast exchange between rotamers is expected to produce the population-averaged chemical shift values and the population-averaged dipolar interactions seen by the NOE experiment. Thus, ROESY analysis reflects the dominating impact of (**6b**-H$^+$)$_1$ but does not exclude the significant population of other major rotamers.

The significant chemical shift difference of the 1^1-H and 1^2-H resonances may reflect their location with respect to the shielding zone of the adjacent 4′-*p*-tolyl group. The resonance located upfield corresponds to the 1^1-H atom that is positioned close to the *p*-tolyl plane. Alternatively, the

involvement of the exposed 1^2-H in interactions via hydrogen bonding with the TFA molecules may be instrumental in the detected chemical shift differentiation.[53,54] The 1^1-H hydrogen encapsulated in the dimeric cleft is expected to have limited access to such hydrogen acceptors.

DFT Studies

The structural formula of **6b**-H^+ shown in Scheme 5 demonstrated merely the projection facilitating a presentation. To account for the ^{1}H NMR characteristics of **6b**-H^+, non-planar structural scaffolds were considered (Figure 4). Consequently, DFT studies were used to visualize the suggested structures of **6b**-H^+ and to assess the preference of the major rotamers with respect to the C2–C3′ bond. Eventually, we realized that the orientation of the aryl substituents is of importance. Geometries of four fundamental rotamers with respect to the C2–C3′ and C(indole)–C(aryl)$_{ipso}$ bonds were optimized at the B3LYP/6-31G** level. Two representative optimized structures are shown in Figure 5. The optimized geometries for two other rotamers are shown in Supporting Information (Figures S30 and S31). The structures are identified by sets of dihedral angles as shown in Table 1. The calculated relative energies, using the B3LYP/6-31G**//B3LYP/6-31G** approach, are gathered in Table 2.

Table 2. Calculated relative energies [kcal mol^{-1}] of the **6b**-H^+ conformers.

Conformer	$E_{rel.}$
(**6b**-H^+)$_1$	0.00
(**6b**-H^+)$_2$	1.00
(**6b**-H^+)$_3$	1.94
(**6b**-H^+)$_4$	1.69

The exact energy ordering has no quantitative significance, as the calculations were performed without a solvent model and feasible interaction with TFA molecules.

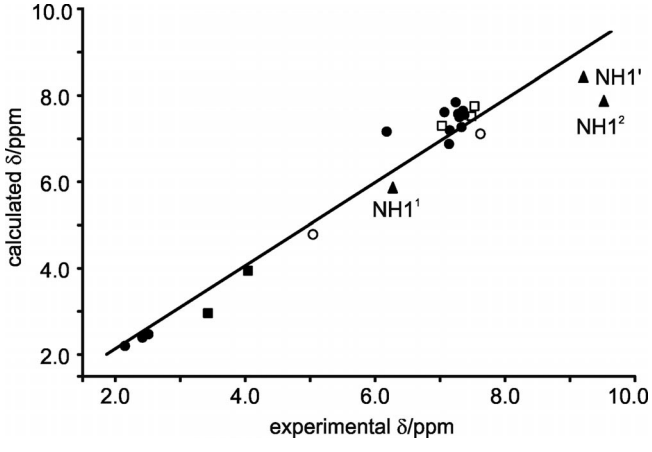

Figure 6. The representative linear correlation between calculated for (**6b**-H^+)$_3$ (GIAO B3LYP/6-31G**) and experimental (rotamer population averaged) values of chemical shifts (▲: NH; ○: 2-H, 2′-H; ■: 3-H; □: 5-H, 6-H, 5′-H, 6′-H; ●: *p*-Tol).

The ^{1}H NMR chemical shifts calculated for **1b** and (**6b**-H^+)$_{1–4}$ by using the GIAO B3LYP/6-31G** method are given in the Supporting Information (Tables S7–S11). There are satisfactory qualitative agreements between the calculated and experimental chemical shifts of the CH and 1′-NH resonances, even though the experimental chemical shifts correspond to rotamer population-averaged values, shown practically for all rotamers (Figure 6; Supporting Information, S33–S35). The experimental chemical shifts of the ammonium unit are well reproduced for the (**6b**-H^+)$_3$ and (**6b**-H^+)$_4$ forms, whereas the marked downfield relocation of 1^2-NH with respect to 1^1-NH has been clearly replicated.

Conclusions

An atypical procedure to construct a fused arene ring around a pyrrole to form 4,7-disubstitued indoles has been elaborated. The indole ring, favorably decorated at the 4,7-positions can be considered as a suitable building block appropriately preorganized to be incorporated in functional polymeric materials containing poly(*p*-phenylene) (PPP), poly(*p*-phenylene vinylene) (PPV), or polythiophenes (PT) backbones.

Experimental Section

General Methods: Dichloromethane and triethylamine were distilled from CaH_2. Solvents like ethanol, *n*-hexane, at least pure grade, were used without purification. Tetrahydrofuran (THF) was purified via pushing through an absorber column (M Braun SPS-800 system). [D_2]Dichloromethane was used as received. [D]Chloroform was prepared directly before using by passing through a small basic alumina column. Inorganic salts were used without purification. Compounds **3b–d**, **4b–d**, **5b–d**, and **2b–d** were synthesized analogically to the previously reported procedure.[29] NMR spectra were measured with Bruker Avance 500 MHz and Bruker Avance 600 MHz spectrometers. ^{1}H and ^{13}C shifts are referenced to the residual resonances of deuterated solvents. 2D NMR spectra were recorded typically with 2048 data points in the *t*2 domain and up to 1024 points in the *t*1 domain with a 1 s recovery delay. Mass spectra (high-resolution and accurate-mass) were recorded with a Bruker microTOF-Q spectrometer by using the electrospray technique.

1,4-Di(*p*-tolyl)-2-butyne-1,4-diol (3b): Yield: 4.9 g, 46%. Cream amorphous solid. Synthesized by a previously reported procedure by using *p*-tolualdehyde instead of benzaldehyde.[29] ^{1}H NMR (600 MHz, $CDCl_3$, 300 K): δ = 7.42 (d, ^3J = 8.1 Hz, 4 H, *o*-Tol), 7.18 (d, ^3J = 7.9 Hz, 4 H, *m*-Tol), 5.52 (d, ^3J = 6.0 Hz, 2 H, 1-H, 4-H), 2.4 (s, 6 H, Me), 2.12 (d, ^3J = 6.0 Hz, 1 H, OH), 2.11 (d, ^3J = 6.0 Hz, 1 H, OH) ppm. ^{13}C NMR (150.90 MHz, $CDCl_3$, 300 K): δ = 138.4, 137.5, 129.3, 126.6, 86.4, 64.6, 21.1 ppm. HRMS (ESI): calcd. for [$C_{18}H_{18}O_2$ + Na]$^+$ 289.1205; found 289.1201.

1,4-Di(*p*-methoxyphenyl)-2-butyne-1,4-diol (3c): Yield: 8.2 g, 69%. Cream amorphous solid. Synthesized by a previously reported procedure by using *p*-anisaldehyde instead of benzaldehyde.[29] ^{1}H NMR (500 MHz, $CDCl_3$, 300 K): δ = 7.46 (d, ^3J = 8.7 Hz, 4 H, *o*-PhOMe), 6.90 (d, ^3J = 8.7 Hz, 4 H, *m*-PhOMe), 5.50 (d, ^3J = 5.6 Hz, 2 H, 1-H, 4-H), 3.80 (s, 6 H, OMe), 2.22 (d, ^3J = 5.6 Hz,

1 H, OH), 2.21 (d, ^3J = 5.6 Hz, 1 H, OH) ppm. ^{13}C NMR (125.76 MHz, $CDCl_3$, 300 K): δ = 159.8, 132.6, 128.1, 114.0, 86.4, 64.3, 55.3 ppm. HRMS (ESI): calcd. for $[C_{18}H_{18}O_4 + Na]^+$ 321.1103; found 321.1096.

1,4-Di(thien-2-yl)-2-butyne-1,4-diol (3d): Yield: 7 g, 70%. Pale brown amorphous solid. Synthesized by a previously reported procedure by using 2-thiophenecarboxaldehyde instead of benzaldehyde.[29] ^{1}H NMR (600 MHz, $CDCl_3$, 300 K): δ = 7.31 (dd, ^3J = 5.0, ^4J = 1.2 Hz, 2 H, 5-Th), 7.19 (m, 2 H, 3-Th), 6.98 (dd, ^3J = 5.0, ^3J = 3.5 Hz, 2 H, 4-Th), 5.75 (br. s, 2 H, 1-H, 4-H), 2.54 (br. s, 2 H, OH) ppm. ^{13}C NMR (150.9 MHz, $CDCl_3$, 300 K): δ = 143.9, 126.8, 126.3, 125.8, 85.1, 60.3 ppm. HRMS (ESI): calcd. for $[C_{12}H_{10}O_2S_2 + Na]^+$ 273.0020, found 273.0025.

1,4-Di(*p*-tolyl)-1,4-di(pyrrol-2-yl)but-2-yne (2b): Yield: 35 mg, 30%. Yellow oil. The first step, the synthesis and purification of the dicobalt complex of 1,4-di(*p*-tolyl)-2-butyne-1,4-diol **3b** (yield: 6.6 g, 95%, red amorphous solid), was analogous to the previously reported procedure for **3a**. The second step, the synthesis and purification of the dicobalt complex of 1,4-di(*p*-tolyl)-1,4-di(pyrrol-2-yl)-but-2-yne **4b** (yield: 1.49 g, 73%, brown-red oil), was analogous to the previously reported procedure for **4a**, except **4b** (main brown-red fraction) was eluted with dichloromethane/hexanes fraction (1:1). The third step, the synthesis and purification of **2b**, was analogous to the previously reported procedure for **2a**. Characterization of **2b**: ^{1}H NMR (600 MHz, CD_2Cl_2, 300 K): δ = 8.18 (br. s, 2 H, NH), 7.28 (d, ^3J = 8.0 Hz, 4 H, *o*-Tol), 7.16 (d, ^3J = 8.0 Hz, 4 H, *m*-Tol), 6.65 (m, 2 H, pyr), 6.08 (m, 2 H, pyr), 5.98 (m, 2 H, pyr), 5.13 (s, 2 H, 1-H, 4-H), 2.33 (s, 6 H, Me) ppm. ^{13}C NMR (150.90 MHz, CD_2Cl_2, 300 K): δ = 139.2 (*p*-Tol), 138.6 (*i*-Tol), 132.7 (α-pyr), 130.9 (*m*-Tol), 128.9 (*o*-Tol), 118.8 (pyr), 110.0 (pyr), 107.6 (pyr), 84.9 (C2, C3), 38.0 (C1, C4), 22.3 (Me) ppm. HRMS (ESI): calcd. for $[C_{26}H_{24}N_2 + H]^+$ 365.2018; found 365.2011.

1,4-Di(*p*-methoxyphenyl)-1,4-di(pyrrol-2-yl)but-2-yne (2c): Yield: 47 mg, 37%. Yellow oil. The first step, the synthesis and purification of the dicobalt complex of 1,4-di(*p*-methoxyphenyl)-2-butyne-1,4-diol **3c** (yield: 6 g, 82%, red amorphous solid), was analogous to the previously reported procedure for **3a**. The second step, the synthesis and purification of the dicobalt complex of 1,4-di(*p*-methoxyphenyl)-1,4-di(pyrrol-2-yl)but-2-yne **4c** (yield: 1.35 g, 63%, brown-red oil), was analogous to the previously reported procedure for **4a**, except **4c** (main brown-red fraction) was eluted with dichloromethane. The third step, the synthesis and purification of **2c**, was analogous to the previously reported procedure for **2a**, except **2c** (second yellow fraction) was eluted with dichloromethane. Characterization of **2c**: ^{1}H NMR (500 MHz, $CDCl_3$, 300 K): δ = 8.06 (br. s, 2 H, NH), 7.31 (d, ^3J = 8.8 Hz, 4 H, *o*-PhOMe), 6.87 (d, ^3J = 8.8 Hz, 4 H, *m*-PhOMe), 6.66 (m, 2 H, pyr), 6.14 (m, 2 H, pyr), 6.00 (m, 2 H, pyr), 5.11 (s, 2 H, 1-H, 4-H), 3.80 (s, 6 H, OMe) ppm. ^{13}C NMR (125.76 MHz, CD_2Cl_2, 300 K): δ = 158.7 (*p*-PhOMe), 132.4 (*i*-PhOMe), 131.2 (α-pyr), 128.7 (*o*-PhOMe), 117.2 (pyr), 114.0 (*m*-PhOMe), 108.5 (pyr), 106.2 (pyr), 83.4 (C2, C3), 55.3 (OMe), 36.0 (C1, C4) ppm. HRMS (ESI): calcd. for $[C_{26}H_{24}N_2O_2]^+$ 396.1837; found 396.1831.

1,4-Di(pyrrol-2-yl)-1,4-di(thien-2-yl)but-2-yne (2d): Yield: 18 mg, 16%. Yellow oil. The first step, the synthesis and purification of the dicobalt complex of 1,4-di(2-thienyl)-2-butyne-1,4-diol **3d** (yield: 6.4 g, 95%, red amorphous solid), was analogous to the previously reported procedure for **3a**. The second step, the synthesis and purification of the dicobalt complex of 1,4-di(pyrrol-2-yl)-1,4-di(2-thienyl)but-2-yne **4d** (yield: 1.35 g, 68%, brown-red oil), was analogous to the previously reported procedure for **4a**, except **4d** (main brown-red fraction) was eluted with dichloromethane/hexanes fraction (1:1). The third step, the synthesis and purification of **2d**, was analogous to the previously reported procedure for **2a**, except a silica gel suspension in dichloromethane in a glass column was purged with nitrogen for 30 min and chromatography was carried out under a nitrogen atmosphere. Characterization of **2d**: ^{1}H NMR (600 MHz, $CDCl_3$, 300 K): δ = 8.17 (2 H, NH), 7.22 (d, ^3J = 5.0 Hz, 2 H, 5-Th), 7.00 (m, 2 H, 3-Th), 6.96 (dd, ^3J = 5.0, ^3J = 3.5 Hz, 2 H, 4-Th), 6.71 (m, 2 H, pyr), 6.18–6.14 (bb, 4 H, pyr), 5.43 (s, 2 H, 1-H, 4-H) ppm. ^{13}C NMR (150.90 MHz, $CDCl_3$, 300 K): δ = 144.0 (2-Th), 129.7 (α-pyr), 126.8 (4-Th), 125.1 (3-Th), 124.8 (5-Th), 117.6 (pyr), 108.6 (pyr), 106.4 (pyr), 82.5 (C2, C3), 32.0 (C1, C4) ppm. HRMS (ESI): calcd. for $[C_{20}H_{16}N_2S_2]^+$ 348.0755; found 348.0739.

4,7-Diphenylindole (1a): Yield: 18 mg, 31%. Brown amorphous solid. Compound **2a** was synthesized by a previously reported procedure.[29] Compound **2a** (59 mg, 0.22 mmol) was dissolved in freshly distilled dichloromethane (25 mL), and the solution was purged with nitrogen gas for 15 min. Then, tifluoroacetic acid (17 μL, 0.22 mmol) was added, and the mixture was stirred under a nitrogen atmosphere for 1 h. Next, triethylamine (31 mL, 0.22 mmol) was added, and the solution was stirred for 30 min. Then, the solvent was evaporated to dryness, and the residue was purified by chromatography on silica gel. The first yellow fraction eluted with dichloromethane was collected to give **1a**. ^{1}H NMR (600 MHz, $CDCl_3$, 300 K): δ = 8.52 (br. s, 1 H, 1-H), 7.75 (d, ^3J = 7.65 Hz, 2 H, 4-*o*), 7.68 (d, ^3J = 7.56 Hz, 2 H, 7-*o*), 7.53 (d, ^3J = 7.5 Hz, 2 H, 7-*m*), 7.5 (d, ^3J = 7.5 Hz, 2 H, 4-*m*), 7.41 (t, ^3J = 7.35 Hz, 2 H, 7-*p*), 7.39 (t, ^3J = 7.35 Hz, 2 H, 4-*p*), 7.32 (d, ^3J = 7.4 Hz, 1 H, 6-H), 7.3 (d, ^3J = 7.4 Hz, 1 H, 5-H), 7.26 (dd, ^3J = 3.3, ^4J = 2.3 Hz 1 H, 2-H), 6.81 (dd, ^3J = 3.3, ^4J = 2.2 Hz, 1 H, 3-H) ppm. ^{13}C NMR (150.90 MHz, $CDCl_3$, 300 K): δ = 141.1 (4-*ipso*), 139.1 (7-*ipso*), 134.1 (7a), 133.8 (4), 129.2 (7-*m*), 128.8 (4-*o*), 128.5 (4-*m*), 128.2 (7-*o*), 127.5 (7-*p*), 127.0 (4-*p*), 126.4 (3a), 124.8 (7), 124.7 (2), 122.3 (6), 120.3 (5), 102.7 (3) ppm. HRMS (ESI): calcd. for $[C_{20}H_{15}N + H]^+$ 270.1283; found 270.1286.

Deuteration of 1a: A solution of **1a** in $CDCl_3$ was placed in an NMR tube (typically a sample of ca. 2 mg of **1a**). Addition of [D]-TFA and D_2O to the solution of **1a** gave **1a**-d_2. ^{1}H NMR (600 MHz, $CDCl_3$, 300 K): δ = 7.75 (d, ^3J = 7.65 Hz, 2 H, 4-*o*), 7.68 (d, ^3J = 7.56 Hz, 2 H, 7-*o*), 7.53 (d, ^3J = 7.5 Hz, 2 H, 7-*m*), 7.5 (d, ^3J = 7.5 Hz, 2 H, 4-*m*), 7.41 (t, ^3J = 7.35 Hz, 2 H, 7-*p*), 7.39 (t, ^3J = 7.35 Hz, 2 H, 4-*p*), 7.32 (d, ^3J = 7.4 Hz, 1 H, 6-H), 7.3 (d, ^3J = 7.4 Hz, 1 H, 5-H), 7.26 (br. s, 1 H, 2-H) ppm.

4,7-Di(*p*-tolyl)indole, 4,7-di(*p*-methoxyphenyl)indole, and 4,7-di(thien-2-yl)indole were prepared analogically to the procedure reported for **1a**.

4,7-Di(*p*-tolyl)indole (1b): Yield: 25 mg, 38%. Brown amorphous solid. ^{1}H NMR (600 MHz, $CDCl_3$, 300 K): δ = 8.51 (br. s, 1 H, 1-H), 7.64 (d, ^3J = 7.98 Hz, 2 H, 4-*o*), 7.6 (d, ^3J = 7.98 Hz, 2 H, 7-*o*), 7.33 (d, ^3J = 7.86 Hz, 2 H, 7-*m*), 7.31 (d, ^3J = 7.92 Hz, 2 H, 4-*m*), 7.28 (d, ^3J = 7.4 Hz, 1 H, 6-H), 7.26 (d, ^3J = 7.4 Hz, 1 H, 5-H), 7.25 (dd, 1 H, 2-H), 6.79 (dd, ^3J = 3.2, ^4J = 2.2 Hz, 1 H, 3-H), 2.44 (s, 3 H, 4-Me or 7-Me), 2.44 (s, 3 H, 4-Me or 7-Me) ppm. ^{13}C NMR (150.90 MHz, $CDCl_3$, 300 K): δ = 138.2 (4-*ipso*), 137.2 (7-*p*), 136.6 (4-*p*), 136.2 (7-*ipso*), 134.1 (7a), 133.5 (4), 129.9 (7-*m*), 129.2 (4-*m*), 128.6 (4-*o*), 128.1 (7-*o*), 126.4 (3a), 124.5 (7), 124.5 (2), 122.2 (6), 120.1 (5), 102.7 (3), 21.2 (Me) ppm. HRMS (ESI): calcd. for $[C_{22}H_{19}N + H]^+$ 298.1596; found 298.1598.

4,7-Di(*p*-methoxyphenyl)indole (1c): Yield: 58 mg, 80%. Brown amorphous solid. ^{1}H NMR (500 MHz, CD_2Cl_2, 300 K): δ = 8.60 (br. s, 1 H, 1-H), 7.67 (d, ^3J = 8.7 Hz, 2 H, 4-*o*), 7.61 (d, ^3J = 8.7 Hz, 2 H, 7-*o*), 7.29 (dd, ^3J = 3.3, ^4J = 2.3 Hz, 1 H, 2-H), 7.24

(d, ^3J = 7.4 Hz, 1 H, 6-H), 7.21 (d, ^3J = 7.4 Hz, 1 H, 5-H), 7.08 (d, ^3J = 8.7 Hz, 2 H, 7-*m*), 7.04 (d, ^3J = 8.7 Hz, 2 H, 4-*m*), 6.77 (dd, ^3J = 3.3, ^4J = 2.3 Hz, 1 H, 3-H), 3.88 (s, 3 H, OMe), 3.87 (s, 3 H, OMe) ppm. ^{13}C NMR (125.76 MHz, CD_2Cl_2, 300 K): δ = 160.8 (7-*p*), 160.5 (4-*p*), 135.7 (7a), 135.2 (4-*ipso*), 134.4 (4), 133.0 (7-*ipso*), 131.2 (4-*o*), 130.8 (7-*o*), 127.9 (3a), 126.2 (2), 125.7 (7), 123.6 (6), 121.4 (5), 116.2 (7-*m*), 115.6 (4-*m*), 103.9 (3), 56.9 (OMe), 56.8 (OMe) ppm. HRMS (ESI): calcd. for $[C_{22}H_{19}NO_2 + H]^+$ 330.1489; found 330.1492.

4,7-Di(thien-2-yl)indole (1d): Yield: 25 mg, 84%. Brown amorphous solid. Compound **2d** (37 mg, 0.11 mmol) was dissolved in freshly distilled dichloromethane (12 mL), and the solution was purged with nitrogen gas for 15 min. Then, trifluoroacetic acid (8 μL, 0.11 mmol) was added, and the mixture was stirred under a nitrogen atmosphere for 30 min. Next, triethylamine (15 mL, 0.11 mmol) was added, and the solution was stirred for 30 min. Then, the solvent was evaporated to dryness, and the residue was purified by chromatography on silica gel. A silica gel suspension in dichloromethane in a glass column was purged with nitrogen for 30 min and chromatography was carried out under a nitrogen atmosphere. The first orange fraction eluted with dichloromethane was collected to give **1d**. ^{1}H NMR (600 MHz, $CDCl_3$, 300 K): δ = 8.77 (br. s, 1 H, 1-H), 7.49 [dd, ^3J = 3.5 Hz, ^4J = 1.2 Hz, 1 H, 4-(3-th)], 7.41 (d, ^3J = 7.4 Hz, 1 H, 5-H or 6-H), 7.40 [dd, ^3J = 3.5 Hz, ^4J = 1.2 Hz, 1 H, 7-(3-th)], 7.38 (d, ^3J = 7.4 Hz, 1 H, 5-H or 6-H), 7.38–7.36 [m, 2 H, 4,7-(5-th)], 7.33 (dd, ^3J = 3.3 Hz, ^4J = 2.1 Hz, 1 H, 2-H), 7.20 [dd, ^3J = 5 Hz, ^3J = 3.5 Hz, 1 H, 7-(4-th)], 7.18 [dd, ^3J = 5 Hz, ^3J = 3.5 Hz, 1 H, 4-(4-th)], 7.04 (dd, ^3J = 3.3 Hz, ^4J = 2.1 Hz, 1 H, 3-H) ppm. ^{13}C NMR (150.90 MHz, $CDCl_3$, 300 K): δ = 143.4 [4-(2-th)], 140.9 [7-(2-th)], 133.7 (4), 128.0 [7-(4-th)], 127.6 [4-(4-th)], 126.9 (3a), 125.9 (7), 125.03 (2), 124.99 [7-(3-th)], 124.9 [4-(3-th)], 124.8 and 124.6 [4,7-(5-th)], 122.1 (5 or 6), 119.9 (5 or 6), 117.9 (7a), 103.2 (3) ppm. HRMS (ESI): calcd. for $[C_{16}H_{11}NS_2 + H]^+$ 282.0406; found 282.0400.

2-(4,7-Diphenylindol-3-yl)-4,7-diphenylindolinium (6a-H$^+$): Evidence of compound by NMR spectroscopy. A solution of **1a** in $CDCl_3$ was placed in an NMR tube (typically a sample of ca. 2 mg of **1a**). Titration of **1a** was carried out with TFA (2.2 M in $CDCl_3$) at 240 K. The progress of the reaction was followed by NMR spectroscopy. ^{1}H NMR (600 MHz, $CDCl_3$, 240 K): δ = 9.55 (t, 1 H, 1-H), 9.32 (d, ^3J = 2.6 Hz, 1 H, 1′-H), 7.68 (d, ^3J = 2.6 Hz, 1 H, 2′-H), 7.63–7.49, 7.48–7.40, 7.36 (d, ^3J = 7.5 Hz, 1 H, 4′-*o*), 7.32 (d, ^3J = 7.4 Hz, 1 H, 5′-H or 6′-H), 7.28–7.23, 7.08 (d, ^3J = 7.4 Hz, 1 H, 5′-H or 6′-H), 7.03 (t, ^3J = 7.5 Hz, 1 H, 4′-*m*), 6.38 (t, ^3J = 7.5 Hz, 1 H, 4′-*p*), 6.07 (br. s, 1 H, 1-H), 5.08 (m, 1 H, 2-H), 4.10 (dd, ^2J = 15.6 Hz, ^3J = 12.3 Hz, 1 H, 3-H), 3.45 (dd, ^2J = 15.6 Hz, ^3J = 6.8 Hz, 1 H, 3-H) ppm. ^{13}C NMR (150.9 MHz, $CDCl_3$, 240 K): δ = 140.1, 138.8, 137.5, 137.4, 134.3, 133.1, 132.1, 132.0, 131.9, 131.1, 129.5, 129.4, 129.2, 128.8, 128.7, 128.4, 128.1–127.9, 126.2, 126.1, 123.4, 122.8, 122.5, 106.2, 63.0, 33.4 ppm. HRMS (ESI): calcd. for $[C_{40}H_{31}N_2]^+$ 539.2482; found 539.2477.

2-(4,7-Di-*p*-tolylindol-3-yl)-4,7-di-*p*-tolylindolinium (6b-H$^+$): Evidence of compound by NMR spectroscopy. A solution of **1b** in $CDCl_3$ was placed in an NMR tube (typically a sample of ca. 2 mg of **1b**). Titration of **1b** was carried out with TFA (2.2 M in $CDCl_3$) at 260 K. The progress of the reaction was followed by NMR spectroscopy. ^{1}H NMR (600 MHz, $CDCl_3$, 260 K): δ = 9.52 (br. s, 1 H, 1-H), 9.21 (d, ^3J = 2.6 Hz, 1′-H), 7.62 (d, ^3J = 2.6 Hz, 2′-H), 7.54 (d, ^3J = 8.0 Hz, 1 H, 5-H), 7.48 (d, ^3J = 8.0 Hz, 2 H, 7′-*o*), 7.37 (d, ^3J = 8.0 Hz, 1 H, 6-H), 7.36–7.29 (8 H, 4-*m*, 7-*m*, 7′-*m* and 4-*o*), 7.28 (d, ^3J = 7.4 Hz, 1 H, 6′-H), 7.24 (d, 1 H, 4′-*o*), 7.15 (d, ^3J = 7.8 Hz, 2 H, 7-*o*), 7.14 (d, 1 H, 4′-*o*), 7.07 (d, ^3J = 7.4 Hz, 1 H, 4′-*m*), 7.03 (d, ^3J = 7.4 Hz, 1 H, 5′-H), 6.27 (br. s, 1 H, 1-H), 6.18 (d, ^3J = 7.4 Hz, 1 H, 4′-*m*), 5.04 (m, 1 H, 2-H), 4.04 (dd, ^2J = 15.5 Hz, ^3J = 12.0 Hz, 1 H, 3-H), 3.43 (dd, ^2J = 15.5 Hz, ^3J = 6.8 Hz, 1 H, 3-H), 2.51 (s, 3 H, 7-Me), 2.43 (s, 3 H, 7′-Me), 2.42 (s, 3 H, 4-Me), 2.15 (s, 3 H, 4′-Me) ppm. ^{13}C NMR (150.9 MHz, $CDCl_3$, 260 K): δ = 139.7, 138.8, 138.6, 138.1, 138.0, 137.5, 134.7, 134.65, 134.6, 133.0, 131.9, 131.81, 131.78, 131.6, 131.2, 130.2, 129.6, 129.5, 129.29, 129.26, 129.2, 128.2–127.7, 126.2, 125.9, 123.5, 122.9, 122.8, 106.6, 63.1, 33.4, 21.27, 21.24, 21.17, 21.1 ppm. HRMS (ESI): calcd. for $[C_{44}H_{39}N_2]^+$ 595.3113; found 595.3120.

2-(4,7-Di-*p*-tolylindol-3-yl)-4,7-di-*p*-tolylindoline (6b): [D_5]Pyridine (30 equiv.) was added to a solution of **6b**-H$^+$ prepared in previous experiment. Compound **6b**-H$^+$ was converted into **6b** at once. ^{1}H NMR (600 MHz, $CDCl_3$, 240 K): δ = 10.74 (s, 1 H, 1-H), 10.70 (s, 1 H, 1′-H), 7.50 (d, ^3J = 7.7 Hz, 1 H), 7.41 (d, ^3J = 7.7 Hz, 1 H), 7.38 (d, ^3J = 7.7 Hz, 2 H), 7.28 (d, ^3J = 2.2 Hz, 1 H), 7.26–6.98, 6.92 (d, ^3J = 7.0 Hz, 1 H), 6.87 (d, 1 H), 6.86 (d, ^3J = 7.4 Hz, 1 H), 6.64 (d, ^3J = 7.9 Hz, 1 H), 6.62 (t, 1 H), 6.44 (d, ^3J = 7.4 Hz, 1 H), 4.72 (dd, ^3J = 11.3 Hz, ^3J = 7.8 Hz, 1 H, 2-H), 3.01 (dd, ^2J = 14.8 Hz, ^3J = 11.3 Hz, 1 H, 3-H), 2.86 (dd, ^2J = 14.8 Hz, ^3J = 7.8 Hz, 1 H, 3-H), 2.31–1.93 ppm.

Structure Analysis: An X-ray quality crystal of **1c** was prepared by diffusion of *n*-hexane into a solution of dichloromethane contained in a tube stored at room temperature. Data were collected at 100 K with an Xcalibur PX-k geometry diffractometer with Mo-K_α radiation (λ = 0.71073 Å). Data were corrected for Lorentz and polarization effects. Crystal data is compiled in Table S1 (Supporting Information). The structure was solved by direct methods with SHELXS-97 and refined by full-matrix least-squares method by using SHELXL-97. Scattering factors were those incorporated in SHELXS-97.[55,56] Hydrogen atoms were fixed in idealized positions using the riding model constraints.

CCDC-879658 (for **1c**) contains the supplementary crystallographic data for this paper. These data can be obtained free of charge from The Cambridge Crystallographic Data Centre via www.ccdc.cam.ac.uk/data_request/cif.

DFT Calculations: DFT calculations were performed with the Gaussian 03 program.[57] Starting geometries were obtained by using molecular mechanics calculations. Geometry optimizations were carried out within unconstrained C1 symmetry. Becke's three parameter exchange functional[58] with the gradient-corrected correlation formula of Lee, Yang, and Parr (B3LYP)[59] was used with the 6-31G** basis set. The structures were found to have converged to a minimum on the potential energy surface; the resulting zero-point vibrational energies were included in the calculation of relative energies. The proton chemical shifts were calculated at the GIAO-B3LYP/6-31G** level for the optimized structures. The Cartesian coordinates for the calculated structures are given in the Supporting Information.

Supporting Information (see footnote on the first page of this article): Tables of computational results (Cartesian coordinates), figures presenting correlations between calculated and experimental ^{1}H NMR chemical shifts, NMR spectroscopic data, crystal data for **1c**.

Acknowledgments

Financial support from the Ministry of Science and Higher Education (Grant N N204 021939) is kindly acknowledged. Quantum chemical calculations were carried out at the Poznań Supercom-

puter Center (Poznań) and Wrocław Supercomputer Center (Wrocław).

[1] D. A. Horton, G. T. Bourne, M. L. Smythe, *Chem. Rev.* **2003**, *103*, 893–930.
[2] J. Weng, H. Omar, K. Kulp, C. Chen, *Mini-Rev. Med. Chem.* **2010**, *10*, 398–404.
[3] V. Sharma, P. Kumar, D. Pathak, *J. Heterocycl. Chem.* **2010**, *47*, 491–502.
[4] K. A. Miller, R. M. Williams, *Chem. Soc. Rev.* **2009**, *38*, 3160–3174.
[5] S. A. Patil, R. Patil, D. D. Miller, *Curr. Med. Chem.* **2009**, *16*, 2531–2565.
[6] D. Bialonska, J. K. Zjawiony, *Mar. Drugs* **2009**, *7*, 166–183.
[7] L. Joucla, L. Djakovitch, *Adv. Synth. Catal.* **2009**, *351*, 673–714.
[8] J. D. Matichak, J. M. Hales, S. Barlow, J. W. Perry, S. R. Marder, *J. Phys. Chem. A* **2011**, *115*, 2160–2168.
[9] Q. Li, Z. Li, C. Ye, J. Qin, *J. Phys. Chem. B* **2008**, *112*, 4928–4933.
[10] Q. D. Liu, M. S. Mudadu, H. Schmider, R. Thummel, Y. Tao, S. I. Wang, *Organometallics* **2002**, *21*, 4743–4749.
[11] Q. Fang, B. Xu, B. Jiang, H. T. Fu, X. Y. Chen, A. Cao, *Chem. Commun.* **2005**, 1468–1470.
[12] Q. Li, J. Zou, J. Chen, Z. Liu, J. Qin, Z. Li, Y. Cao, *J. Phys. Chem. B* **2009**, *113*, 5816–5822.
[13] R. Zostautiene, G. Krucaite, J. Simokaitiene, J. Grazulevicius, V. Y. Lai, W. Wang, J. Jou, S. Grigalevicius, *Dyes Pigm.* **2011**, *91*, 177–181.
[14] Q. Peng, X. Liu, Y. Qin, J. Xu, M. Li, L. Dai, *J. Mater. Chem.* **2011**, *21*, 7714–7722.
[15] E. Zhou, S. Yamakawa, Y. Zhang, K. Tajima, C. Yang, K. Hashimoto, *J. Mater. Chem.* **2009**, *19*, 7730–7737.
[16] G. R. Humphrey, J. T. Kuethe, *Chem. Rev.* **2006**, *106*, 2875–2911.
[17] M. Bandini, A. Eichholzer, *Angew. Chem.* **2009**, *121*, 9786; *Angew. Chem. Int. Ed.* **2009**, *48*, 9608–9644.
[18] J. Barluenga, F. Rodriguez, F. J. Fananas, *Chem. Asian J.* **2009**, *4*, 1036–1048.
[19] G. Bartoli, G. Bencivenni, R. Dalpozzo, *Chem. Soc. Rev.* **2010**, *39*, 4449–4465.
[20] E. M. Beck, M. J. Gaunt, *Top. Curr. Chem.* **2010**, *292*, 85–121.
[21] R. Vicente, *Org. Biomol. Chem.* **2011**, *9*, 6469–6480.
[22] S. Cacchi, G. Fabrizi, *Chem. Rev.* **2011**, *111*, R215–R283.
[23] D. F. Taber, P. K. Tirunahari, *Tetrahedron* **2011**, *67*, 7195–7210.
[24] K. R. Rathikrishnan, V. K. Indirapriyadharshini, S. Ramakrishna, R. Murugan, *Tetrahedron* **2011**, *67*, 4025–4030.
[25] J. Moskal, A. M. van Leusen, *J. Org. Chem.* **1986**, *51*, 4131–4139.
[26] N. Asao, H. Aikawa, *J. Org. Chem.* **2006**, *71*, 5249–5253.
[27] M. Yamashita, K. Hirano, T. Satoh, M. Miura, *Org. Lett.* **2009**, *11*, 2337–2340.
[28] H. Huang, J. Li, W. Zhao, Y. Mei, Z. Duan, *Org. Biomol. Chem.* **2011**, *9*, 5036–5038.
[29] E. Nojman, A. Berlicka, L. Szterenberg, L. Latos-Grażyński, *Inorg. Chem.* **2012**, *51*, 3247–3260.
[30] J. Krupowicz, K. Sapiecha, *Roczniki Chemii* **1973**, *47*, 1729–1730.
[31] J. Krupowicz, K. Sapiecha, R. Gaszczyk, *Roczniki Chemii* **1974**, *48*, 2067–2068.
[32] R. F. Lockwood, K. M. Nicholas, *Tetrahedron Lett.* **1977**, *18*, 4163–4166.
[33] S. Padmanabhan, K. M. Nicholas, *Tetrahedron Lett.* **1983**, *24*, 2239–2242.
[34] S. L. Schreiber, M. T. Klimas, T. Sammakia, *J. Am. Chem. Soc.* **1987**, *109*, 5749–5759.
[35] K. M. Nicholas, *Acc. Chem. Res.* **1987**, *20*, 207–214.
[36] B. J. Teobald, *Tetrahedron* **2002**, *58*, 4133–4170.
[37] I. Omae, *Appl. Organomet. Chem.* **2007**, *21*, 318–344.
[38] K. M. Bromfield, H. Graden, N. Ljungdahl, N. Kann, *Dalton Trans.* **2009**, 5051–5061.
[39] M. Pawlicki, L. Latos-Grażyński in *Handbook of Porphyrin Science: With Applications to Chemistry, Physics, Materials Science Engineering, Biology and Medicine* (Eds.: K. M. Kadish, K. M. Smith, R. Guilard), World Scientific Publishing, Singapore, **2010**, vol. 2, pp. 104–192.
[40] T. D. Lash, *Eur. J. Org. Chem.* **2007**, 5461–5481.
[41] A. Chen, J. W. Zou, W. N. Zhao, *Acta Crystallogr., Sect. E: Struct. Rep. Online.* **2007**, *63*, O3229–U3679.
[42] Y. Xie, Y. Zhao, B. Qian, L. Yang, C. Xia, H. Huang, *Angew. Chem. Int. Ed.* **2011**, *50*, 5681–5685.
[43] K. M. Smith in *Porphyrins and Metalloporphyrins* (Ed.: K. M. Smith), Elsevier, Amsterdam **1975**, pp. 29–58.
[44] B. J. Littler, Y. Ciringh, J. S. Lindsey, *J. Org. Chem.* **1999**, *64*, 2864–2872.
[45] G. R. Geier III, B. J. Littler, J. S. Lindsey, *J. Chem. Soc. Perkin Trans. 2* **2001**, 701.
[46] R. L. Hinman, C. P. Bauman, *J. Org. Chem.* **1964**, *29*, 2437–2348.
[47] A. R. Katritzky, A. F. Pozharski, *Handbook of Heterocyclic Chemistry*, Pergamon, Amsterdam, **2000**.
[48] a) H. F. Hodson, G. F. Smith, *J. Chem. Soc.* **1957**, 3544–3545; b) G. F. Smith, *Adv. Heterocycl. Chem.* **1963**, *2*, 287–309.
[49] P. Barbaro, C. Bianchini, A. Meli, M. Moreno, F. Vizza, *Organometallics* **2002**, *21*, 1430–1437.
[50] J. Bergman, E. Koch, B. Pelcman, *Tetrahedron Lett.* **1995**, *36*, 3945–3948.
[51] W. E. Noland, C. F. Hammer, *J. Org. Chem.* **1960**, *25*, 1525–1535.
[52] G. Quartarone, L. Ronchin, C. Tortato, A. Vavasori, *Int. J. Chem. Kinet.* **2009**, *41*, 107–112.
[53] M. Stępień, B. Szyszko, L. Latos-Grażyński, *J. Am. Chem. Soc.* **2010**, *132*, 3140–3152.
[54] P. J. Chmielewski, L. Latos-Grażyński, *J. Chem. Soc. Perkin Trans. 2* **1995**, 503–509.
[55] G. M. Sheldrick, *SHELXL97–Program for Crystal Structure Refinement*, University of Göttingen, Göttingen, **1997**.
[56] G. M. Sheldrick, *SHELXS97–Program for Crystal Structure Solution*, University of Göttingen, Göttingen, **1997**.
[57] M. J. Frisch, G. W. Trucks, H. B. Schlegel, G. E. Scuseria, M. A. Robb, J. R. Cheeseman, J. A. Montgomery Jr., T. Vreven, K. N. Kudin, J. C. Burant, J. M. Millam, S. S. Iyengar, J. Tomasi, V. Barone, B. Mennucci, M. Cossi, G. Scalmani, N. Rega, G. A. Petersson, H. Nakatsuji, M. Hada, M. Ehara, K. Toyota, R. Fukuda, J. Hasegawa, M. Ishida, T. Nakajima, Y. Honda, O. Kitao, H. Nakai, M. Klene, X. Li, J. E. Knox, H. P. Hratchian, J. B. Cross, V. Bakken, C. Adamo, J. Jaramillo, R. Gomperts, R. E. Stratmann, O. Yazyev, A. J. Austin, R. Cammi, C. Pomelli, J. W. Ochterski, P. Y. Ayala, K. Morokuma, G. A. Voth, P. Salvador, J. J. Dannenberg, V. G. Zakrzewski, S. Dapprich, A. D. Daniels, M. C. Strain, O. Farkas, D. K. Malick, A. D. Rabuck, K. Raghavachari, J. B. Foresman, J. V. Ortiz, Q. Cui, A. G. Baboul, S. Clifford, J. Cioslowski, B. B. Stefanov, G. Liu, A. Liashenko, P. Piskorz, I. Komaromi, R. L. Martin, D. J. Fox, T. Keith, M. A. Al Laham, C. Y. Peng, A. Nanayakkara, M. Challacombe, P. M. W. Gill, B. Johnson, W. Chen, M. W. Wong, C. Gonzales, J. A. Pople, *Gaussian 03*, revision C.02., Gaussian, Inc., Wallingford, CT, **2004**.
[58] A. D. Becke, *Phys. Rev. A* **1988**, *38*, 3098–3100.
[59] C. Lee, W. Yang, R. G. Parr, *Phys. Rev. B* **1988**, *37*, 785–789.

Received: May 14, 2012
Published Online: ■

EurJOC European Journal of Organic Chemistry

Disubstituted Indoles

An alternative route for the construction of indole derivatives is described. 4,7-Diarylindoles and 4,7-di(thien-2-yl)indole were synthesized by applying a strategy where the fused benzene ring was built on the existing pyrrole.

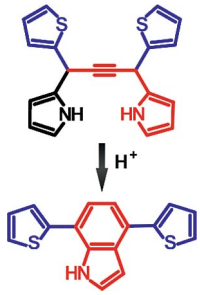

Keywords: Heterocycles / Dimerization / Rearrangement / NMR spectroscopy

